AD-A193 276 PARAMAGNETIC POINT DEFECTS IN BORON-IMPLANTED 1/1
HG97CD03TE..(U) AEROSPACE CORP EL SEGUNDO CA CHEMISTRY
AND PHYSICS LAB R C BOWMAN ET AL. 01 FEB 88
UNCLASSIFIED TR-0086(6945-07)-4 SD-TR-88-03 F/G 7/2 NL

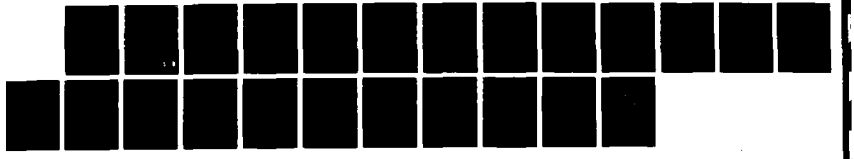

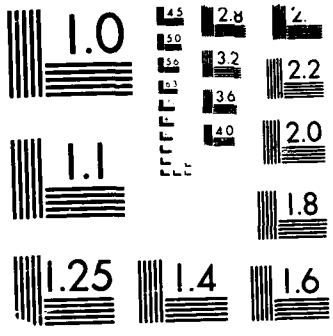

MICROCOPY RESOLUTION TEST CHART
STANDARDS

AD-A193 276

REPORT SD-TR-88-03

Paramagnetic Point Defects in Boron-Implanted $Hg_{0.7}\ Cd_{0.3}\ Te$

R. C. BOWMAN, JR.
Chemistry and Physics Laboratory
Laboratory Operations
The Aerospace Corporation
El Segundo, CA 90245

E. L. VENTURINI
Sandia National Laboratories
Albuquerque, NM 87185

and

S. N. WITT
Division of Chemistry and Chemical Engineering
California Institute of Technology
Pasadena, CA 91125

1 February 1988

Prepared for

SPACE DIVISION
AIR FORCE SYSTEMS COMMAND
Los Angeles Air Force Station
P.O. Box 92960, Worldway Postal Center
Los Angeles, CA 90009-2960

DTIC
ELECTE
MAR 1 1 1988
S D
H

APPROVED FOR PUBLIC RELEASE;
DISTRIBUTION UNLIMITED

88 3 03 051

This report was submitted by The Aerospace Corporation, El Segundo, CA 90245, under Contract No. F04701-85-C-0086 with the Space Division, P.O. Box 92960, Worldway Postal Center, Los Angeles, CA 90009-2960. It was reviewed and approved for The Aerospace Corporation by S. Feuerstein, Director, Chemistry and Physics Laboratory.

Lt Walter E. Leyland/CNDA was the project officer for the Mission-Oriented Investigation and Experimentation (MOIE) Program.

This report has been reviewed by the Public Affairs Office (PAS) and is releasable to the National Technical Information Service (NTIS). At NTIS, it will be available to the general public, including foreign nationals.

This technical report has been reviewed and is approved for publication. Publication of this report does not constitute Air Force approval of the report's findings or conclusions. It is published only for the exchange and stimulation of ideas.

Walter E Leyland

WALTER E. LEYLAND, Lt, USAF
MOIE Project Officer
SD/CNDA

Raymond M Leong

RAYMOND M. LEONG, Major, USAF
Deputy Director, AFSTC West Coast Office
AFSTC/WCO OL-AB

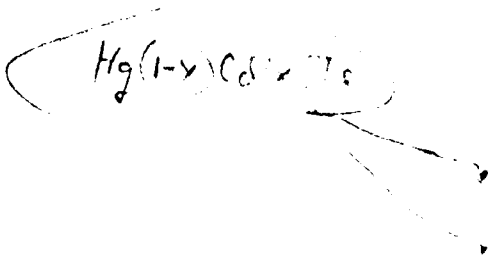

UNCLASSIFIED

SECURITY CLASSIFICATION OF THIS PAGE

A193 276

REPORT DOCUMENTATION PAGE

1a. REPORT SECURITY CLASSIFICATION Unclassified	1b. RESTRICTIVE MARKINGS
2a. SECURITY CLASSIFICATION AUTHORITY	3. DISTRIBUTION / AVAILABILITY OF REPORT Approved for public release; distribution unlimited.
2b. DECLASSIFICATION / DOWNGRADING SCHEDULE	
4. PERFORMING ORGANIZATION REPORT NUMBER(S) TR-0086(6945-07)-4	5. MONITORING ORGANIZATION REPORT NUMBER(S) SD-TR- 88-03
6a. NAME OF PERFORMING ORGANIZATION The Aerospace Corporation Laboratory Operations 6b OFFICE SYMBOL (If applicable)	7a. NAME OF MONITORING ORGANIZATION Space Division
6c. ADDRESS (City, State, and ZIP Code) El Segundo, CA 90245	7b ADDRESS (City, State, and ZIP Code) Los Angeles Air Force Station Los Angeles, CA 90009-2960
8a. NAME OF FUNDING / SPONSORING ORGANIZATION 8b OFFICE SYMBOL (If applicable)	9. PROCUREMENT INSTRUMENT IDENTIFICATION NUMBER F04701-85-C-0086
8c. ADDRESS (City, State, and ZIP Code)	10 SOURCE OF FUNDING NUMBERS PROGRAM ELEMENT NO. / PROJECT NO. / TASK NO / WORK UNIT ACCESSION NO.

11. TITLE (Include Security Classification)
Paramagnetic Point Defects in Boron-Implanted $Hg_{0.7}Cd_{0.3}Te$

12 PERSONAL AUTHOR(S) Bowman, Robert C.; Venturini, E. L., Sandia National Laboratories; Witt, S. N., California Institute of Technology

13a. TYPE OF REPORT	13b. TIME COVERED FROM ____ TO ____	14. DATE OF REPORT (Year, Month, Day)	15 PAGE COUNT
		1 February 1988	19

16. SUPPLEMENTARY NOTATION

17 COSATI CODES		
FIELD	GROUP	SUB-GROUP

18 SUBJECT TERMS (Continue on reverse if necessary and identify by block number)
Cadmium Telluride; Ion Implantation; Defects in Semiconductors; IR Detector Materials; Electron Paramagnetic Resonance; Mercury Cadmium Telluride

19 ABSTRACT (Continue on reverse if necessary and identify by block number)

The initial observations of electron paramagnetic resonance (EPR) spectra from $Hg_{0.7}Cd_{0.3}Te$ and CdTe after implantation with boron ions are described in this report. Sharp and nearly isotropic EPR signals with the free electron g-values were easily detected at low temperatures (≤ 78 K) when the boron ion implant dose was 1×10^{16} ions/cm^2 or larger. For identical implant conditions, more intense signals and narrower peaks were obtained from $Hg_{0.7}Cd_{0.3}Te$ samples than from CdTe samples. However, the g-factors for all implanted $Hg_{1-x}Cd_xTe$ samples appear to be equivalent and are similar to the values reported for the dangling-bond defects in other ion-implanted semiconductors. The EPR spectra produced by the boron implants do not correspond to either the degenerate conduction electron bands that form in ion-implanted $Hg_{1-x}Cd_xTe$ or to the shallow donor states previously found in chemically doped CdTe. When implanted crystals are cooled below 4 K, partially resolved, two-component

20 DISTRIBUTION / AVAILABILITY OF ABSTRACT	21 ABSTRACT SECURITY CLASSIFICATION	
☐ UNCLASSIFIED/UNLIMITED ☒ SAME AS RPT ☐ DTIC USERS	Unclassified	
22a NAME OF RESPONSIBLE INDIVIDUAL	22b TELEPHONE (Include Area Code)	22c OFFICE SYMBOL

DD FORM 1473, 84 MAR 83 APR edition may be used until exhausted. All other editions are obsolete

SECURITY CLASSIFICATION OF THIS PAGE

UNCLASSIFIED

19. Abstract (Continued)

lineshapes are observed at some orientations. Increasing the temperature causes these two-component lines to collapse into nearly Lorentzian lineshapes with temperature-dependent widths. This behavior is consistent with a thermally activated process by which the paramagnetic spins hop between different locations. KEYWORDS: [illegible] TELLURIDE; [illegible] CADMIUM TELLURIDE.

PREFACE

We wish to thank Professor S. I. Chan for making the electron paramagnetic resonance spectrometer available at Caltech, R. E. Robertson for assistance with the samples, and Dr. J. F. Knudsen for the ion implants.

DTIC COPY INSPECTED

Accession For
NTIS GRA&I ☑
DTIC TAB ☐
Unannounced ☐
Justification
By
Distribution/
Availability Codes
Dist | Avail and/or Special
A-1

CONTENTS

PREFACE..... 1

I. INTRODUCTION..... 7

II. EXPERIMENTAL BACKGROUND..... 9

III. EFFECTS OF BORON ION IMPLANTS..... 13

REFERENCES..... 21

TABLES

1. Properties of $Hg_{1-x}Cd_xTe$ Samples Used for Boron Implantation Studies..... 10

2. Summary of EPR Parameters for $^{11}B^+$ Ion-Implanted $Hg_{1-x}Cd_xTe$ Crystals..... 15

FIGURES

1. Comparison of Lorentzian and Gaussian Least-Squares Fits to the EPR Derivative Lineshape Obtained at 4 K from the $^{11}B^+$ Implanted $Hg_{0.68}Cd_{0.32}Te$ Sample (H6) When the Magnetic Field Is Along the <100>-Direction..... 14

2. Changes in the 2 K EPR Derivative Lineshapes as the $^{11}B^+$ Implanted $Hg_{0.68}Cd_{0.32}Te$ Crystal Is Rotated ± 45 deg from the <100>-Direction..... 17

3. Comparison of Two-Line and One-Line Fits to +45 deg Orientation of Implanted $Hg_{0.68}Cd_{0.32}Te$ Sample at Different Temperatures..... 18

I. INTRODUCTION

Ion implants are commonly used during the fabrication of $Hg_{1-x}Cd_xTe$ infrared (IR)-photodiode devices. Without further processing, these implants always appear[1-3] to create an n-type layer in $Hg_{1-x}Cd_xTe$. Although the nature of these donor states has not been definitively established, the states are widely believed[1-3] to be implant-induced damage "defects" and not the implanted atoms. However, thermal anneals can electrically activate some implanted species to reveal[3] donor (e.g., In) or acceptor (e.g., P) behavior. The properties of implanted boron atoms, which should be donors when substituted on the metal sites in $Hg_{1-x}Cd_xTe$, remain very controversial. Although it is unclear[2,3] whether the implanted boron ions play any direct role as active donors in the formation of the n-p junction, boron implants have been widely used[1] to produce photodiodes. More complete information on the interactions of boron implants with damage defects or impurities is needed to resolve the specific contributions of boron atoms to the electrical properties of implanted $Hg_{1-x}Cd_xTe$.

Electron paramagnetic resonance (EPR) spectroscopy, which is also known as electron spin resonance (ESR), is a powerful method to characterize point defects in elemental and compound semiconductors. Analyses of the experimental EPR parameters, such as the g-factor constant, fine structure constant, and hyperfine coefficients, can unequivocally identify paramagnetic defects or impurities in many instances.[4] Although EPR studies have been performed on numerous II-VI compound semiconductors,[5-7] relatively few studies have been performed on the $Hg_{1-x}Cd_xTe$ system. Whereas characteristic EPR spectra have been reported for transition metals,[8] shallow donors,[9] and deep donors[10,11] in CdTe, only two papers[12,13] have presented EPR results for the ternary $Hg_{1-x}Cd_xTe$ alloys. Consequently, EPR experiments have been performed on boron-implanted CdTe and $Hg_{0.7}Cd_{0.3}Te$ crystals to determine whether donor states or other paramagnetic species have been created by the implantation process. Rather intense EPR signals with "free-electron" spin characteristics have been detected at low temperatures after boron implants of 10^{16} ions/cm^2

or larger. Although the specific defects responsible for these new signals cannot yet be identified, the spectral properties are similar to those of the EPR spectra for the dangling-bond centers previously found in ion-implanted silicon[14] can GaP.[15] Thermal anneals up to 300°C do not significantly alter the concentration of the paramagnetic defects in boron-implanted $Hg_{1-x}Cd_xTe$, although some minor changes in the EPR spectra are apparent.

II. EXPERIMENTAL BACKGROUND

Two X-band* spectrometers are used for the EPR measurements: a Varian E-line spectrometer and a homemade homodyne spectrometer. A Varian E-line spectrometer has a slotted window in one wall of the microwave cavity, which permitted in situ illumination of samples at temperatures down to about 5 K when used with an Air Products Heli-Tran liquid transfer system. The homemade homodyne spectrometer, with the microwave cavity in a cold helium gas flow, permitted EPR measurements to be made in the dark at temperatures as low as 2 K. Prior calibrations of the homodyne spectrometer provided accurate g-value determinations as well as semiquantitative estimates (i.e., uncertainties of about 25-50%) of the spin concentrations.

The $Hg_{1-x}Cd_xTe$ samples used in the EPR experiments were nominally undoped bulk single crystals with volumes between 10 and 50 mm^3. The semi-insulating (SI) CdTe crystals had been purchased from II-VI, Inc. The p-type $Hg_{0.7}Cd_{0.3}Te$ crystals had been obtained from Cominco and New England Research Corporation (NERC). Although the orientations for the major crystal faces were known, in some cases several $Hg_{0.7}Cd_{0.3}Te$ wafers were sliced randomly. Properties of crystal samples that were subsequently implanted with boron are presented in Table 1. EPR measurements were performed on all the $Hg_{1-x}Cd_xTe$ materials prior to implantation. One of the CdTe crystals (sample C1) exhibited EPR spectra that correspond to the paramagnetic transition metals Fe^{+3} and Co^{+2} previously seen by other researchers.[8] No EPR signals have been observed from other $Hg_{1-x}Cd_xTe$ samples listed in Table 1. When these crystals were cooled to temperatures below 15 K, in-situ illumination with ultraviolet (UV)-filtered, IR-filtered, and an unfiltered 250 W xenon lamp had no noticeable effect upon the EPR signals for any $Hg_{1-x}Cd_xTe$ sample. In particular, there was no evidence for the $g \approx 2.235 - 2.5$ or $g = 3.0$

---

*An X-band system operates at a nominal resonant microwave frequency of 9 GHz.

Table 1. Properties of $Hg_{1-x}Cd_xTe$ Samples Used for Boron Implantation Studies

ID Label	X	Implant Face	Crystal Source	Type	Carrier Contents[a] ($10^{15}cm^{-3}$)	Paramagnetic Species Seen Before Implants
C1	1.00	<111>	II-VI, Inc.	SI[b]	-	Fe^{+3}, Co^{+2}
C2	1.00	<100>	II-VI, Inc.	SI	-	None
H5	0.32	<110>	Cominco	P	9	None
H6	0.32	<110>	Cominco	P	60	None
H7	0.31	Random	NERC[c]	P	13	None

[a]From 77 K Hall data provided by the vendors.

[b]Semi-insulating (i.e., resistivity $>10^6$ ohm-cm at room temperature).

[c]New England Research Corporation.

paramagnetic centers recently reported for undoped p-type $Hg_{0.7}Cd_{0.3}Te$ by Jones et al.[13]

The acceptor levels for the $Hg_{0.7}Cd_{0.3}Te$ crystals in Table 1 vary by more than a factor of 6. Although numerous experimental factors can preclude[4,16] the observation of EPR spectra, considerable effort was made to alter the present operating conditions so that paramagnetic signals could be detected. Cavity tuning and stability difficulties were encountered with the narrower band gap $Hg_{0.7}Cd_{0.3}Te$ samples even before the ion implants. The implants will generate highly conductive surface layers that result in well-known[16] skin-depth effects. However, any significant concentrations of paramagnetic centers would have been detected if they had been present.

The boron ($^{11}B^+$) ions were implanted into the $Hg_{1-x}Cd_xTe$ samples with a Model 400 MPR-Veeco/AI ion-implanter system. The implants were performed at room temperature with low ion dose rates to minimize inadvertent heating effects. No new EPR signals were observed from various $Hg_{1-x}Cd_xTe$ crystals implanted with boron that had energies from 40 to 250 keV. The total boron doses in these crystals was up to 2×10^{15} ions/cm^2. Because thresholds for the observations of implant-induced EPR spectra had been reported for other semiconductors,[14,15] a heavy four-stage implant (2.5×10^{15} B^+ ions/cm^2 at 100, 200, 300, and 400 keV) was performed to produce a total dose of 1×10^{16} B^+ ions/cm^2. Samples from all of the crystals in Table 1 were simultaneously implanted under the conditions just described. The conditions are expected[17] to produce a fairly uniform ^{11}B distribution (although the mean boron content will decrease with distance from the implant surface) more than 1 μm into the $Hg_{1-x}Cd_xTe$ crystals. The actual n-p junction will probably lie deeper than the boron implant,[18] but its position has not been determined. We intended to produce sufficient volumes of boron implant and damage regions to detect any paramagnetic centers with the available EPR equipment.

III. EFFECTS OF BORON ION IMPLANTS

After a four-stage, room temperature $^{11}B^{+}$ implant to produce a total dose of 1×10^{16} ions/cm^2, new EPR spectra were observed from $Hg_{1-x}Cd_xTe$ samples listed in Table 1. Figure 1 exhibits a representative first derivative spectrum for an implanted $Hg_{0.7}Cd_{0.3}Te$ crystal when it was cooled to 5 K. Similar signals were obtained between 2 and 78 K, although cavity tuning became more difficult at higher temperatures. As illustrated in Fig. 1, Lorentzian lineshapes give much better fits than Gaussian curves to experimental traces obtained at 5 K or higher temperatures. Similar results were found for the implant-induced signals from the other implanted $Hg_{1-x}Cd_xTe$ samples. In several cases, significantly improved fits occurred by including a second Lorentzian line with a narrower width. The inhomogeneous distribution of the paramagnetic centers created during implantation may be responsible for the need to include a second component to the lineshapes. The g-factor constants, the peak-to-peak linewidths (ΔH_{pp}), and the paramagnetic spin concentrations normalized to sample weights that were derived from the fitted EPR spectra are summarized in Table 2. The actual densities of paramagnetic centers are much greater than indicated in Table 2. The defects are presumably confined to regions affected by the boron implants, which only penetrate approximately 1 μm into the crystals. The dimensions of the damaged regions are currently unknown. However, the effective densities are estimated to be between 10^{17} and 10^{19} spins/cm^3, if the paramagnetic defects are assumed to be distributed from 1.0 to 10 μm below the surface.

The g-factor constants in Table 2 are considered to be equivalent for all the implanted $Hg_{1-x}Cd_xTe$ samples and are also nearly identical to the free-electron g-factor (g_e) of 2.0023. Although these g-factors are slightly anisotropic, a positive g-factor shift ($g-g_e$) of 5 (1) $\times 10^{-4}$ was obtained. Ion implants have previously produced paramagnetic "dangling-bond" defects in Si and GaP with isotropic g-factors of 2.0059 and 2.0032, respectively.[14,15] These dangling-bond centers are usually attributed[19] to localized electronic states formed when covalent bonds are broken. Although the character of a

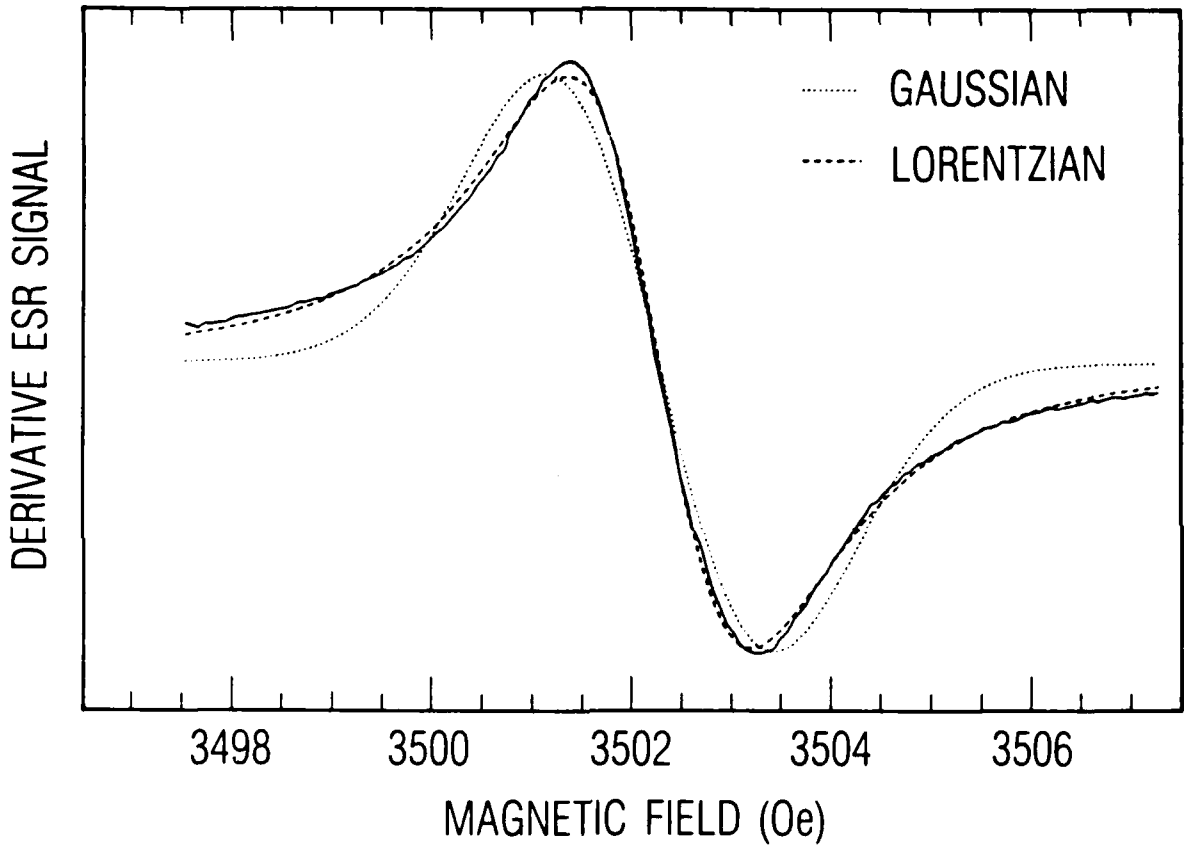

Fig. 1. Comparison of Lorentzian and Gaussian Least-Squares Fits to the EPR Derivative Lineshape Obtained at 4 K from the $^{11}B^{+}$ Implanted $Hg_{0.68}Cd_{0.32}Te$ Sample (H6) When the Magnetic Field Is Along the <100>-Direction

Table 2. Summary of EPR Parameters for $^{11}B^{+}$ Ion-Implanted $Hg_{1-x}Cd_xTe$ Crystals[a]

Sample Label	X	T (K)	Annealing Conditions	g-factor	ΔH_{pp} (G)	Nominal Concentration (spins/gm)
C1	1.00	5	As implanted	2.0030(1) 2.0028(1)	6.7 2.6	2.3×10^{14} 0.3×10^{14}
C3	1.00	5	As implanted	2.0028(1)	6.8	5.9×10^{14}
H5	0.32	2	As implanted	2.0028(2)	3.5	-
		2	200°C, 1 hr	2.0028(1)	2.5	-
		2	300°C, 1 hr	2.0029(1) 2.0023(1)	4.6 1.7	4.0×10^{14} 1.1×10^{14}
H6	0.32	4	As implanted	2.0028(1)	1.8	3.5×10^{15}
H7	0.31	5	As implanted	2.0029(1) 2.0028(1)	6.0 2.4	6.7×10^{14} 0.4×10^{14}

[a]The total dose was 1×10^{16} ions/cm^2, and T corresponds to the temperature during the EPR measurements. Magnetic fields are approximately perpendicular to the implanted crystal face for each sample.

dangling-bond defect in an ionic II-VI semiconductor such as CdTe is not obvious, the g-factors in Table 2 for boron-implanted $Hg_{1-x}Cd_xTe$ are consistent with these defects. In contrast, the g-factors for boron-implanted CdTe samples are distinctly different from the $g \approx 1.7$ reported by other researchers[9] for shallow donor states in chemically doped CdTe. Low temperature (~ 10 K) illuminations of all the boron-implanted $Hg_{1-x}Cd_xTe$ crystals also did not generate $g \approx 1.7$ EPR signals associated with shallow donors. Furthermore, the measured temperature dependencies of the EPR intensities for boron-implanted $Hg_{1-x}Cd_xTe$ samples exhibit an inverse temperature behavior expected for isolated unpaired spins rather than the temperature independent intensities found[16] for conduction electrons. Hence, the EPR spectra produced by boron implants do not directly correspond to the degenerate conduction bands commonly seen[1-3] in implanted HgCdTe. Whereas deep donors usually have[20] small shifts in their g-factors, their presence also gives rise to hyperfine splittings in the EPR spectra, as has been noted previously[10,11] in doped CdTe. Isolated boron deep donor states should produce distinctive hyperfine patterns for both the ^{10}B and ^{11}B isotopes. However, the EPR spectra for boron-implanted $Hg_{1-x}Cd_xTe$ do not indicate these hyperfine splittings. Electron spin-exchange effects[4] between closely spaced paramagnetic centers as well as rapid hopping motions of the spins[20] can eliminate these splittings and produce unsplit and narrowed Lorentzian lines, as are observed from the implanted crystals. The smallest ΔH_{pp} value occurs for the H6 sample with the largest concentration of these paramagnetic centers, which is consistent with the electron spin exchange mechanism.

When the $^{11}B^+$ implanted $Hg_{09.7}Cd_{0.3}Te$ crystals are cooled below approximately 4 K, partially resolved two-component lineshapes are observed for some orientations, as shown in Fig. 2. Although these anisotropic lineshapes could be caused by hyperfine interactions, they cannot be readily interpreted from the natural distribution of the Hg,Cd, or Te isotopes, or from the expected quadruplet for an isolated ^{11}B center. Consequently, the two EPR components that are clearly seen in Fig. 2 could result from two (or more) independent defect centers with slightly different g-factors. Figure 3 illustrates the collapse of the two-component line for the implanted

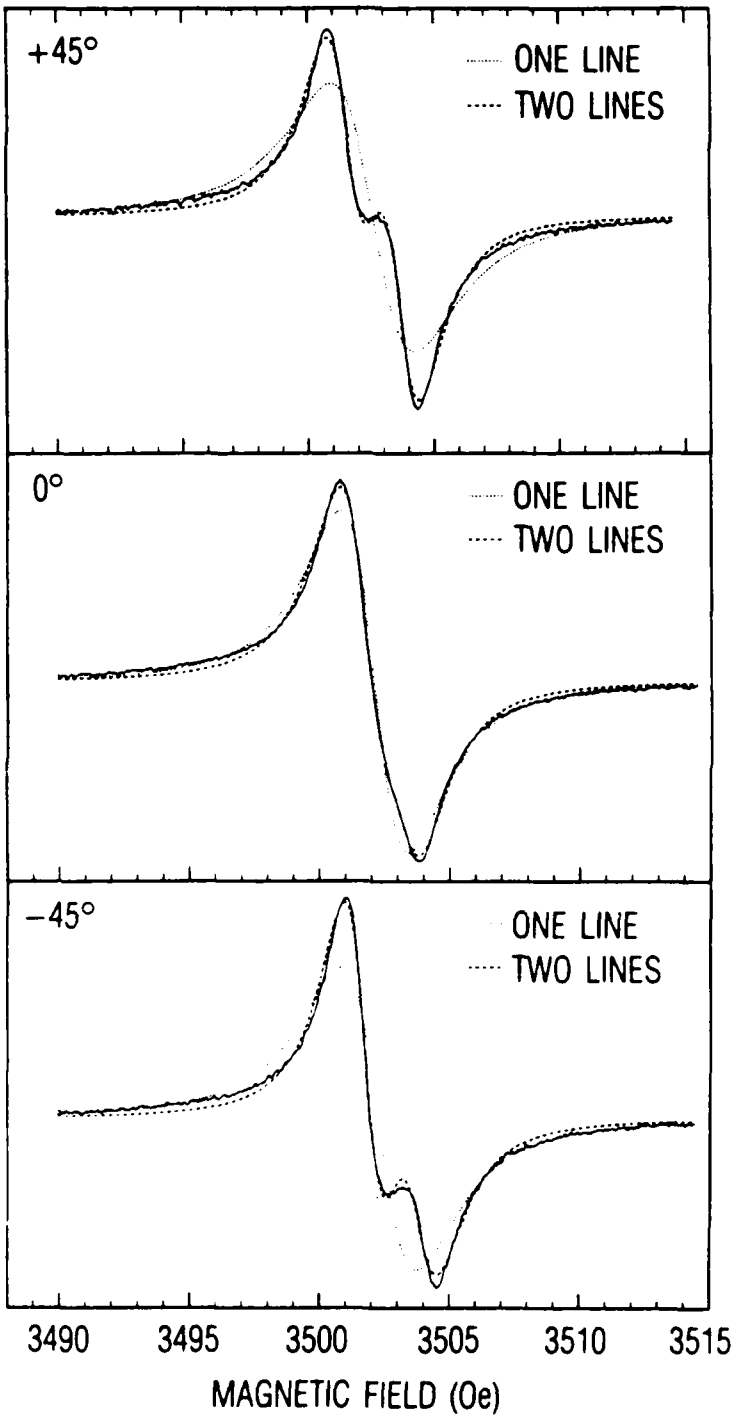

Fig. 2. Changes in the 2 K EPR Derivative Lineshapes as the $^{11}B^{+}$ Implanted $Hg_{0.68}Cd_{0.32}Te$ Crystal Is Rotated ± 45 deg from the <100>-Direction

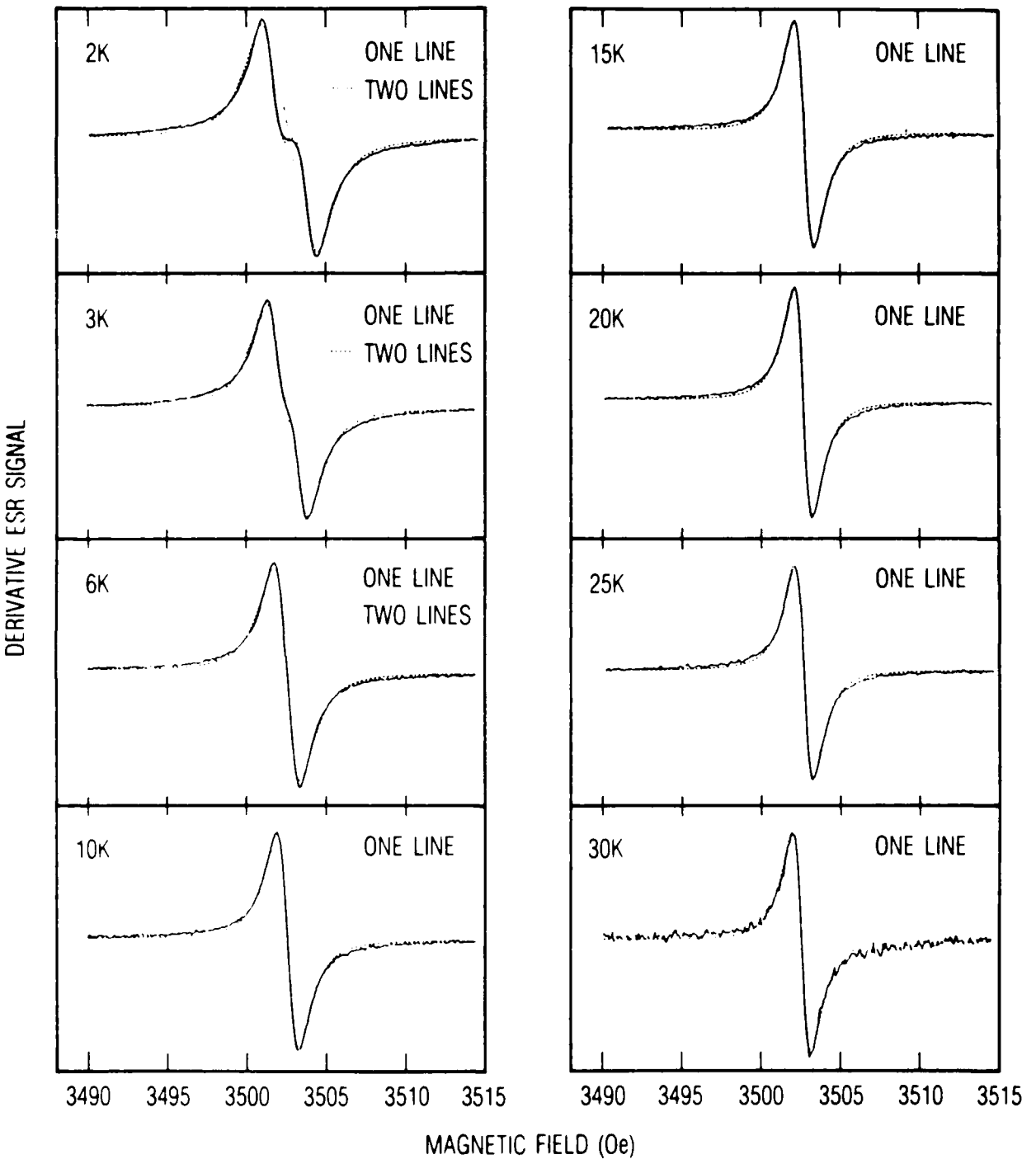

Fig. 3. Comparisons of Two-Line and One-Line Fits to +45 deg Orientation of Implanted $Hg_{0.68}Cd_{0.32}Te$ Sample at Different Temperatures. For temperatures above 6 K, the two-line fits cannot be distinguished from the one-line fits and are not shown.

$Hg_{0.68}Cd_{0.32}Te$ sample H6 into a single peak as the temperature is raised. A symmetric and nearly Lorentzian lineshape is found above 6 K, where ΔH_{pp} values systematically decrease from 1.7 to 1.2 g as the temperature increases to 30 K. This behavior for ΔH_{pp} could be caused by a thermally activated process where the paramagnetic spins hop between two or more different locations. Although the identities of these defects cannot be established from the available data, closely spaced but independent centers would be required to produce the collapse of the EPR lineshape shown in Fig. 3. Similar changes in the low-temperature lineshapes were observed from the other implanted $Hg_{1-x}Cd_xTe$ samples, although the linewidths were generally too large to give the resolutions shown in Figs. 2 and 3. The simultaneous presence of broad and narrow lines obscured these anisotropic lineshape separations for some samples. However, the ΔH_{pp} reduction with increasing temperature is reproduced by all implanted samples.

Studies of thermal anneals on the EPR spectra generated by the $^{11}B^+$ implants were initiated. One hour anneals up to 300°C do not cause significant changes in the g-factors or signal intensities. However, as indicated in Table 2, some changes in lineshapes and ΔH_{pp} values are noted after these anneals. Because only minor alterations in the paramagnetic defect distributions were produced by these anneals, which are known[1-3,13,18] to remove various defects from implanted $Hg_{1-x}Cd_xTe$, the behavior of the EPR signals does not appear to be related to these particular defects. Further experiments that evaluate $^{10}B^+$ implants at different conditions and doses, as well as more varied anneals, are in progress to help establish the microscopic identities of the paramagnetic centers created in $Hg_{1-x}Cd_xTe$ by boron implants. These results will be reported elsewhere.

REFERENCES

1. M. B. Reine, A. K. Sood, and T. J. Tredwell, in Semiconductors and Semimetals - Vol. 18 Mercury Cadmium Telluride, ed. R. K. Willardson and A. C. Beer, Academic, New York (1981), p. 201.

2. G. L. Destefanis, Nucl. Instrum. Meth. 209/210, 567 (1983).

3. T. W. Sigmon, Nucl. Instrum. Meth. B 7/8, 402 (1985).

4. J. E. Wertz and J. R. Bolton, Electron Spin Resonance-Elementary Theory and Practical Applications, McGraw-Hill, New York (1972).

5. R. S. Title, in Physics and Chemistry of II-VI Compounds, ed. M. Aven and J. S. Prener, American Elsevier, New York (1967), p. 265.

6. J. Schneider, II-VI Semiconducting Compounds, ed. D. G. Thomas, Benjamin, New York (1967), p. 40.

7. J. W. Corbett, R. L. Kleinhenz, and N. D. Wilsey, in Defects in Semiconductors, ed. J. Narayan and T. Y. Tan, North-Holland, New York (1981), p. 1.

8. A. Zunger, Solid State Phys. 39, 275 (1986).

9. K. Saminadayar, D. Galland, and E. Molva, Solid State Commun. 49, 627 (1984); and K. Saminadayar, J. M. Francou, and J. L. Pautrat, J. Crystal Growth 72, 236 (1985).

10. R. C. DuVarney and A. K. Garrison, Phys. Rev. B12, 10 (1975).

11. G. Brunthaler, W. Jantsch, U. Kaufmann, and J. Schneider. Phys. Rev. B31, 1239 (1985).

12. A. K. Koh, D. J. Miller, and C. T. Grainger, Phys. Rev. B29, 4904 (1984).

13. C. E. Jones et al., J. Vac. Sci. Technol. A3, 131 (1985).

14. B. L. Crowder, R. S. Title, M. H. Brodsky, and G. D. Pettit, Appl. Phys. Lett. 16, 205 (1970); G. Gotz, W. Karthe, B. Schnabel, and N. Sobolev, Phys. Stat. Sol. (a) 50, K209 (1978).

15. T. Matsumori, K. Miyazaki, and S. Shigetomi, Appl. Phys. Lett. 42, 521 (1983).

16. R. S. Alger, Electron Paramagnetic Resonance: Techniques and Applications, Interscience, New York (1968).

17. H. Ryssel, K. Muller, J. Biersack, W. Kruger, G. Lang, and F. Jahnel, Phys. Stat Sol. (a) 57, 619 (1980).

18. L. O. Bubulac, J. Cryst. Growth 72, 478 (1985).

19. M. H. Brodsky and R. S. Title, Phys. Rev. Lett. 23, 581(1969); P. A. Thomas, H. H. Brodsky, D. Kaplan, and D. Lepine, Phys. Rev. B. 18, 3059 (1978).

20. C. Gonzalez, D. Block, R. T. Cox, and A. Herve, J. Cryst. Growth 59, 357 (1982).

LABORATORY OPERATIONS

The Aerospace Corporation functions as an "architect-engineer" for national security projects, specializing in advanced military space systems. Providing research support, the corporation's Laboratory Operations conducts experimental and theoretical investigations that focus on the application of scientific and technical advances to such systems. Vital to the success of these investigations is the technical staff's wide-ranging expertise and its ability to stay current with new developments. This expertise is enhanced by a research program aimed at dealing with the many problems associated with rapidly evolving space systems. Contributing their capabilities to the research effort are these individual laboratories:

Aerophysics Laboratory: Launch vehicle and reentry fluid mechanics, heat transfer and flight dynamics; chemical and electric propulsion, propellant chemistry, chemical dynamics, environmental chemistry, trace detection; spacecraft structural mechanics, contamination, thermal and structural control; high temperature thermomechanics, gas kinetics and radiation; cw and pulsed chemical and excimer laser development including chemical kinetics, spectroscopy, optical resonators, beam control, atmospheric propagation, laser effects and countermeasures.

Chemistry and Physics Laboratory: Atmospheric chemical reactions, atmospheric optics, light scattering, state-specific chemical reactions and radiative signatures of missile plumes, sensor out-of-field-of-view rejection, applied laser spectroscopy, laser chemistry, laser optoelectronics, solar cell physics, battery electrochemistry, space vacuum and radiation effects on materials, lubrication and surface phenomena, thermionic emission, photosensitive materials and detectors, atomic frequency standards, and environmental chemistry.

Computer Science Laboratory: Program verification, program translation, performance-sensitive system design, distributed architectures for spaceborne computers, fault-tolerant computer systems, artificial intelligence, microelectronics applications, communication protocols, and computer security.

Electronics Research Laboratory: Microelectronics, solid-state device physics, compound semiconductors, radiation hardening; electro-optics, quantum electronics, solid-state lasers, optical propagation and communications; microwave semiconductor devices, microwave/millimeter wave measurements, diagnostics and radiometry, microwave/millimeter wave thermionic devices; atomic time and frequency standards; antennas, rf systems, electromagnetic propagation phenomena, space communication systems.

Materials Sciences Laboratory: Development of new materials: metals, alloys, ceramics, polymers and their composites, and new forms of carbon; nondestructive evaluation, component failure analysis and reliability; fracture mechanics and stress corrosion; analysis and evaluation of materials at cryogenic and elevated temperatures as well as in space and enemy-induced environments.

Space Sciences Laboratory: Magnetospheric, auroral and cosmic ray physics, wave-particle interactions, magnetospheric plasma waves; atmospheric and ionospheric physics, density and composition of the upper atmosphere, remote sensing using atmospheric radiation; solar physics, infrared astronomy, infrared signature analysis; effects of solar activity, magnetic storms and nuclear explosions on the earth's atmosphere, ionosphere and magnetosphere; effects of electromagnetic and particulate radiations on space systems; space instrumentation.

END

DATE

FILMED

DTIC

JULY 88